Electronic Seismologist

A Computational Tool for Ground-Motion Simulations Incorporating Regional Crustal Conditions

Yuxiang Tang[*1,2], Nelson Lam[2,3], and Hing-Ho Tsang[3,4]

Abstract

This article introduces a computational tool, namely ground-motion simulation system (GMSS), for generating synthetic accelerograms based on stochastic simulations. The distinctive feature of GMSS is that it has two independently developed upper-crustal models (expressed in the form of shear-wave velocity profiles), which have been built into the program for deriving the frequency-dependent crustal factors, and one of these models was originally developed by the authors. GMSS also has provisions to allow the user to specify their own preferred crustal profile. Sufficient details of both crustal models (forming part of the seismological model) and the accelerogram simulation methodology are presented herein in one article, to allow any person who has programming skills (on a user-friendly platform such as MATLAB, see Data and Resources), to develop their computational tools to implement any further innovations in crustal modeling for direct engineering applications. Crustal properties deep into bedrock can only be accounted for implicitly by conventional ground-motion prediction equation (GMPE) as much depends on the region where the ground motion was recorded. This limitation of existing GMPEs poses a challenge to engineering in regions that are not well represented by any strong-motion database. Toward the end of this article, readers are enlightened with the potential transdisciplinary utility of using GMSS, to facilitate the retrieval and scaling of accelerograms sourced from a database of real earthquake records through the construction of a conditional mean spectrum.

Cite this article as Tang, Y., N. Lam, and H.-H. Tsang (2020). A Computational Tool for Ground-Motion Simulations Incorporating Regional Crustal Conditions, *Seismol. Res. Lett.* **92**, 1129–1140, doi: 10.1785/0220200222.

Introduction

This article introduces a computational tool, namely ground-motion simulation system (GMSS), written in MATLAB, for generating synthetic accelerograms, for a predefined earthquake scenario (as defined by magnitude and distance). The accelerogram simulation methodology adopts the stochastic approach involving seismological modeling, which has been continuously developed for almost four decades. A review of the makeup of the model and its latest update is presented in The Makeup of the Seismological Model section.

A distinctive feature of GMSS is that it presents a choice of two crustal shear-wave velocity (SWV) models, which can be used to characterize regional, or site-specific, crustal conditions kilometers deep into bedrock, as presented in the Model SWV Profiles section. The ability of this new computational tool to incorporate state-of-the-art modeling of the SWV of the regional upper crust is not paralleled by any existing software. This feature of GMSS will enable stochastic simulations to be applied to any region, including those with a paucity of ground-motion data provided that the crustal conditions are known. Presenting this software in MATLAB would also allow readers to make modifications to the program, to suit individual needs.

A step-by-step illustration of the simulation process is presented in the Ground-Motion Simulation Methodology of GMSS section. Verifications by benchmarking against simulations from a widely used software, namely Stochastic-Method SIMulation (SMSIM), are also shown in the Verification of GMSS, by Benchmarking against SMSIM section. The potential utility of synthetic accelerograms in engineering applications is discussed toward the end of this article, in The Potential Utility of GMSS section.

Neither the seismological model nor GMSS can model multiple reflections of seismic waves that are trapped inside a layer of soil sediments overlying bedrock. Thus, 1D dynamic

1. School of Civil Engineering, Guangzhou University, Guangzhou, China; 2. Department of Infrastructure Engineering, The University of Melbourne, Melbourne, Victoria, Australia; 3. Bushfire and Natural Hazards Cooperative Research Centre, Melbourne, Victoria, Australia; 4. Centre for Sustainable Infrastructure, Swinburne University of Technology, Melbourne, Australia

*Corresponding author: tangyuxiang56@gmail.com

analysis of the soil sediments (by a program like SHAKE or DEEPSOIL) is required, to take into account the aforementioned phenomenon. GMSS may be used to generate excitations transmitted from the bedrock at the soil–rock interface, for input into SHAKE or DEEPSOIL. GMSS is accordingly used for simulating ground motions on the rock surface.

The Makeup of the Seismological Model

This section provides a listing of key expressions that have been developed over many years of research to construct the seismological model, which is essentially algebraic expressions for predicting the frequency content of seismic waves generated by an earthquake expressed in terms of the Fourier amplitude spectrum (FAS). The basic functional form of a seismological model is as defined as follows:

$$\mathrm{E}(\mathbf{M}_0,\mathbf{R},f)=\mathrm{S}(\mathbf{M}_0,f)\times\mathrm{G}(\mathbf{R})\times\mathrm{P}(f,\mathbf{R})\times\mathrm{Am}(f)\times\mathrm{An}(f)\times\mathrm{I}(f)^n, \tag{1}$$

in which $\mathrm{E}(\mathbf{M}_0, \mathbf{R}, f)$ is the predicted FAS of the seismic waves reaching a site, which is at a distance $\mathbf{R}$ from the source in unit of kilometers; $\mathbf{M}_0$ is seismic moment in unit of dyn · cm; f is frequency of ground motion in Hertz. $\mathrm{S}(\mathbf{M}_0, f)$ is source factor; $\mathrm{G}(\mathbf{R})$ is geometric spreading factor; $\mathrm{P}(f, \mathbf{R})$ is anelastic whole path attenuation factor; $\mathrm{Am}(f)$ is upper-crustal amplification factor; $\mathrm{An}(f)$ is upper-crustal attenuation factor; $\mathrm{I}(f) = 2\pi f$ is shape factor; if $n = 0$, predictions are expressed in FAS for acceleration; $n = -1$ for velocity; and $n = -2$ for displacement ($n = 0$ is the default value adopted in this study. Among the earliest contribution to the construction of this framework is the work of Boore (1983).

Source factors

The earliest version of the source factor, as proposed by Brune (1970), is defined by equation (2):

$$\mathrm{S}(\mathbf{M}_0,f)=(2\pi f)^2\frac{C\mathbf{M}_0}{(1+(f/f_c)^2)}, \tag{2}$$

in which C is the mid-crust scaling factor, as defined by equation (3) (Atkinson, 1993):

$$C=\frac{R_pFV}{4\pi\rho_0\beta_0^3R_0}, \tag{3}$$

in which $R_0 = 1$ km; R_p is radiation pattern factor (= 0.55) averaged over a suitable range of azimuths and takeoff angles; F is free-surface amplification factor (= 2.0) for shear waves; V is factor defining the partitioning of shear-wave energy into two horizontal components ($= 1/\sqrt{2}$); ρ_0 and β_0 are the density and SWV in the vicinity of the source, and the units are g/cm^3 and km/s, respectively.

Seismic moment $\mathbf{M}_0$ is related to moment magnitude by equation (4) (Hanks and Kanamori, 1979; Boore, Alessandro, and Abrahamson, 2014):

$$\mathbf{M}=0.67\log(\mathbf{M}_0)-10.7, \tag{4}$$

in which f_c is corner frequency as defined by equation (5) after Brune (1970):

$$f_c=4.9\times10^6\beta_0\left(\frac{\Delta\sigma}{\mathbf{M}_0}\right)^{1/3}, \tag{5}$$

in which β_0 is SWV in km/s, and $\Delta\sigma$ is stress parameter in bars.

For large magnitude ($\mathbf{M} > 6$) earthquakes, the source factor, as defined by equation (6), features two corner frequencies, as presented in (Atkinson and Boore, 1995):

$$\mathrm{S}(\mathbf{M}_0,f)=(2\pi f)^2\mathrm{C}\mathbf{M}_0\left[\frac{1-\varepsilon}{1+(f/f_a)^2}+\frac{\varepsilon}{1+(f/f_b)^2}\right], \tag{6}$$

Parameters are defined by equation (7a–c) for eastern North America (ENA) conditions:

$$\log\varepsilon=2.52-0.637\mathbf{M}, \tag{7a}$$

$$\log f_a=2.41-0.533\mathbf{M}, \tag{7b}$$

$$\log f_b=1.43-0.188\mathbf{M}. \tag{7c}$$

The alternative finite-fault version of the seismological model has also been developed (e.g., Motazedian and Atkinson, 2005). Details are not provided herein. It has been demonstrated in Boore (2009) and Yenier and Atkinson (2014) that the point-source model and the finite-fault source model can deliver similar predictions, by incorporating what is known as the pseudodepth factor (or finite-fault factor) "h_{FF}" into the point-source model. The phenomenon of ground-motion saturation in areas that are close to the fault source is hence accounted for. The functional form of h_{FF} is shown in equation (8), for stable continent conditions (Boore *et al.* 2010):

$$h_{\mathrm{FF}}=10^{-0.405+0.235\mathbf{M}}. \tag{8}$$

The generalized additive double-corner frequency (ADCF) source model, which was introduced more recently in Boore, Alessandro, and Abrahamson (2014), as presented in equation (9), relates the value of f_b to the Brune's single-corner frequency parameter f_c:

$$f_b=\sqrt{[f_c^2-(1-\varepsilon)f_a^2]/\varepsilon}. \tag{9}$$

TABLE 1
Shear-Wave Velocity (SWV) Model Profiles (Boore and Joyner, 1997)

Generic Rock		Generic Hard Rock	
Depth (km)	**SWV (km/s)**	**Depth (km)**	**SWV (km/s)**
$Z \le 0.001$	0.245	0.0	2.768
$0.001 < Z \le 0.03$	$2.206Z^{0.272}$	0.05	2.808
$0.03 < Z \le 0.19$	$3.5426Z^{0.407}$	0.1	2.847
$0.19 < Z \le 4.0$	$2.505Z^{0.199}$	0.2	2.922
$4.0 < Z \le 8.00$	$2.927Z^{0.086}$	0.5	3.122
—	—	0.75	3.260
—	—	$0.75 < Z \le 2.2$	$3.324Z^{0.067}$
—	—	$2.2 < Z \le 8.0$	$3.447Z^{0.0209}$

Given equation (9), the ADCF source spectrum at high frequencies is hence controllable by stress parameter $\Delta\sigma$, as for f_c. The other parameters of the double-corner frequency model f_a and ε can be determined in the same manner, as was done previously. The rest of ADCF may be constrained by the use of equation (7a,b), as recommended in Atkinson and Boore (1995), for ENA conditions, or equations (10) and (11), as recommended in Atkinson and Silva (2000), for western North America conditions:

$$\log \varepsilon = 0.605 - 0.255\mathbf{M}, \tag{10}$$

$$\log f_a = 2.181 - 0.496\mathbf{M}. \tag{11}$$

A review of source models developed for ENA can be found in Boore (2015).

Path factors

There are two path factors for defining the rate of decrease in the ground-motion amplitude with increasing distance: (i) geometrical spreading factor and (ii) anelastic attenuation factor. The geometrical factor is typically defined by equation (12a) within a distance of at least 50 km, but equation (12b) has also been recommended in the literature (e.g., Atkinson and Boore, 2014):

$$G(\mathbf{R}) = \mathbf{R}^{-1}, \tag{12a}$$

$$G(\mathbf{R}) = \mathbf{R}^{-1.3}. \tag{12b}$$

Anelastic attenuation for characterizing loss of energy along the wave travel path has been incorporated into the seismological model through the whole path anelastic attenuation factor $P(f, \mathbf{R})$ which is of the form shown in equation (13):

$$P(f, \mathbf{R}) = Q_o f^n. \tag{13}$$

A review of the two parameters appearing in equation (13) —Q_o and n—can be found in Chandler *et al.* (2006). The determination of the value of the two path factors from field recordings can be affected significantly by trade-offs. It is, therefore, important to adopt compatible values, as recommended by the same literature reference.

Upper-crustal modification factors

A seismic wavefront propagating from a high to low SWV medium will become amplified, as observed from instrumental records in deep drillholes in active seismic areas (Abercrombie, 1997). The amplification factor can be expressed in the form of equation (14):

$$\mathrm{Am}(f) = \sqrt{\frac{\rho_0 \beta_0}{\tilde{\rho}_z \tilde{\beta}_z}}, \tag{14}$$

in which ρ_0 and β_0 are density and SWV in the vicinity of the source; and are time-averaged density, and SWV over a depth corresponding to the quarter wavelength. In this study, the units of ρ_0 and β_0 are g/cm^3 and km/s, respectively.

Values of and can be found using equation (15a,b), respectively:

$$\tilde{\rho}_Z = \left(\int_0^{z(f)} \rho(Z)\mathrm{d}Z\right)/Z(f), \tag{15a}$$

$$\tilde{\beta}_Z = Z(f)/\left(\int_0^{z(f)} \frac{1}{\beta(Z)}\mathrm{d}Z\right), \tag{15b}$$

in which $\rho(Z)$ and $\beta(Z)$ is density and SWV at depth Z. This method of approximation is known as the "Quarter

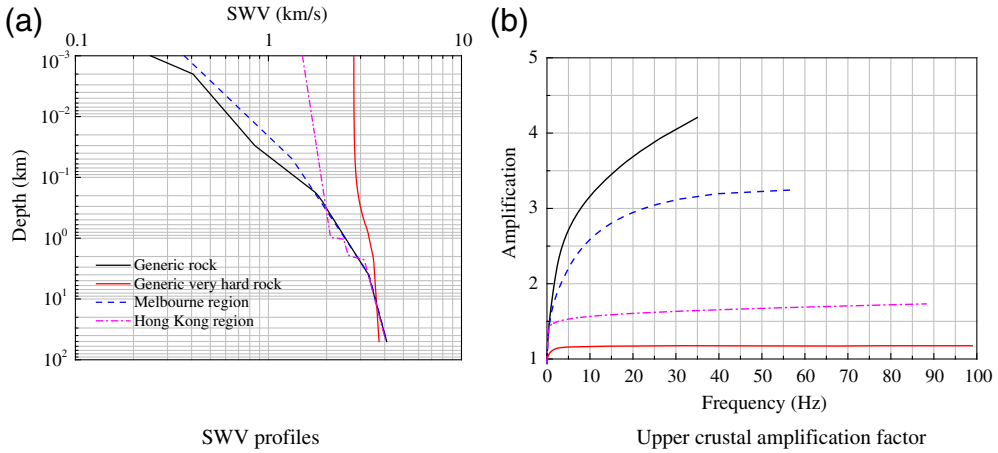

Figure 1. Shear-wave velocity (SWV) profiles and the frequency-dependent amplitude factors. (a) SWV profiles and (b) upper-crustal amplification factor. The color version of this figure is available only in the electronic edition.

Wavelength Approximation (QWA)" method, which is represented by equation (16) (Boore, 2013):

$$Z = \frac{1}{4}\tilde{\beta}/f. \tag{16}$$

Combining equations (15a,b) and (16) results in equation (17):

$$f(Z) = 1/[4\int_0^{Z(f)} \frac{1}{\beta(Z)}\,\mathrm{d}Z]. \tag{17}$$

The upper-crustal amplification factor so calculated is consistent with field observations (Chen, 2000; Boore, 2003).

Another important upper-crustal effect is the upper-crustal attenuation factor, which is to model the path-independent energy loss of the seismic waves. The attenuation factor $\mathrm{An}(f)$ can be represented in two different forms, as shown by equation (18a,b), respectively:

$$\mathrm{An}(f) = [1 + (f/f_{\max})^8]^{-1/2}, \tag{18a}$$

$$\mathrm{An}(f) = \exp(-\pi\kappa_0 f). \tag{18b}$$

Model SWV Profiles

SWV model based on interpolations between generic profiles

Model SWV profiles for generic rock (GR) conditions, typical of California, and generic very hard rock (GHR) conditions, typical of ENA, have been developed by Boore and Joyner (1997). These profiles are defined in Table 1. The time-averaged SWV at the upper 30 m of the soil sediment (V_{S30}) for GR and GHR profiles has the V_{S30} value equal to 0.62 and 2.78 km/s, respectively.

The slowness parameter $S(Z)$ introduced in Boore (2016) is defined by equation (19):

$$S(Z) = \frac{1}{\beta(Z)}. \tag{19}$$

The slowness profile can be derived from linear interpolation of the two generic models (GR and GHR) through the use of equation (20):

$$S(Z) = (1-\varepsilon')S_1(Z) + \varepsilon' S_2(Z), \tag{20}$$

in which $S_1(Z)$ and $S_2(Z)$ are the slowness of the GR and GHR sites at depth Z (in km). Weight coefficient ε' can be determined by setting the average slowness equal to the desired value of $\bar{S}_D$; the value of ε' can be determined using equation (21):

$$\varepsilon' = \frac{\bar{S}_D - \bar{S}_1}{\bar{S}_2 - \bar{S}_1}, \tag{21}$$

in which $\bar{S}_1$ and $\bar{S}_2$ are the average slowness of GR and GHR over the upper 30 m of the crust.

Geology-based SWV model

Several geology-based SWV model profiles incorporating the variation of upper-crustal conditions have been proposed in Chandler *et al.* (2005) and updated by Tang (2019), based on information reported in the CRUST1.0 database, refer Table 2 for the listing of the details. Meanwhile, the model profile of crustal density has been presented in Brocher (2005). Refer Figure 1a,b for the model profiles and upper-crustal amplification factor that have been developed in the case studies of Melbourne Region and Hong Kong Region (for areas within 50 km distance from the two city centers), along with the profiles and amplification factors of the GR and GHR sites.

Ground-Motion Simulation Methodology of GMSS

The GMSS computational tool, as introduced in this article, was written in MATLAB for generating synthetic accelerograms by stochastic simulations of the seismological model, as introduced in The Makeup of the Seismological Model section.

TABLE 2
Intraregional Shear-Wave Velocity (SWV) Model Profiles

Case	Depth Range (km)	β (km/s)
Case 1 ($Z_S \geq 2$)	$0 < Z \leq 0.2$	$\beta_{0.03}(Z/0.03)^{0.3297}$
	$0.2 < Z \leq 2$	$\beta_{0.2}(Z/0.2)^{0.1732}$
	$2 < Z \leq Z_S$	$\beta_2(Z/2)^{0.1667}$
	$Z_S < Z \leq Z_C$	$\beta_{ZC}(Z/Z_C)^n$
	$Z_C < Z$	$\beta_8(Z/8)^{0.0833}$
Case 2 ($0.2 < Z_S < 2 \leq Z_C$)	$Z \leq 0.2$	$\beta_{0.03}(Z/0.03)^{0.3297}$
	$0.2 < Z \leq Z_S$	$\beta_{0.2}(Z/0.2)^{0.1732}$
	$Z_S < Z \leq Z_C$	$\beta_{ZC}(Z/Z_C)^n$
	$Z_C < Z$	$\beta_8(Z/8)^{0.0833}$
Case 3 ($0.2 < Z_S < Z_C \leq 2$)	$0 < Z \leq 0.2$	$\beta_{0.03}(Z/0.03)^{0.3297}$
	$0.2 < Z \leq Z_S$	$\beta_{0.2}(Z/0.2)^{0.1732}$
	$Z_S < Z \leq Z_C$	$\beta_{ZC}(Z/Z_C)^n$
	$Z_C < Z \leq 2$	$\beta_2(Z/2)^{0.0899}$
	$2 < Z$	$\beta_8(Z/8)^{0.0833}$
Case 4 ($Z_S < 0.2 < 2 \leq Z_C$)	$0 < Z \leq Z_S$	$\beta_{ZI}(Z/Z_I)^{0.3297}$
	$Z_S < Z \leq Z_C$	$\beta_{ZC}(Z/Z_C)^n$
	$Z_C < Z$	$\beta_8(Z/8)^{0.0833}$
Case 5 ($Z_S < 0.2 < Z_C \leq 2$)	$Z \leq Z_S$	$\beta_{ZI}(Z/Z_I)^{0.3297}$
	$Z_S < Z \leq Z_C$	$\beta_{ZC}(Z/Z_C)^n$
	$Z_C < Z \leq 2$	$\beta_2(Z/2)^{0.0899}$
	$2 < Z$	$\beta_8(Z/8)^{0.0833}$
Case 6 ($Z_C \leq 0.2$)	$0 < Z \leq Z_S$	$\beta_{ZI}(Z/Z_I)^{0.3297}$
	$Z_S < Z \leq Z_C$	$\beta_{ZC}(Z/Z_C)^n$
	$Z_C < Z \leq 0.2$	$\beta_{0.2}(Z/0.2)^{0.2463}$
	$0.2 < Z \leq 2$	$\beta_2(Z/2)^{0.0899}$
	$2 < Z$	$\beta_8(Z/8)^{0.0833}$

Z_S and Z_C are thickness of upper sediment layer and total sediment layers, respectively; $\beta_{0.03}$, $\beta_{0.2}$, β_2 and β_8 are the SWV values at the depth of 0.03, 0.2, 2, and 8 km, repectively; β_{ZS} and β_{ZC} are the V_S value at the depth of Z_S and Z_C respectively; and $Z_I = \min(Z_S, 0.03)$.

A key feature of GMSS is that the computational procedures can be executed in a transparent manner. A step-by-step illustration is provided herein. The procedure, as a whole, is presented at a glance in Figure 2.

The step-by-step illustration of GMSS programming is stated in the following subsections.

Generation of Gaussian white noise and filter

Gaussian white noise is first generated using a random number generator that is built into MATLAB. The white noise is band-limited from "df" (which is reciprocal of the total duration of the simulated time series) at the lower end to $(N/2 - 1)$ df (the Nyquist frequency) at the higher end, in which N is the number of timesteps in the simulation. A four-level acausal Butterworth filter with a "band-pass" form, as used in the Pacific Earthquake Engineering Research Center (PEER) Next Generation Attenuation-East Project (NGA-East) Database, is adopted (Goulet *et al.*, 2014) in GMSS. In addition, according to Boore and Akkar (2003), the acausal filter is preferred for the calculation of response spectra, because the results are not dependent on the selected filter frequency.

Construction of window function

A window function win(t), as defined by equation (22), is applied to modulate the signal in the time domain:

$$\mathrm{st}(t) = \mathrm{win}(t) \times \mathrm{nt}(t), \tag{22}$$

in which nt(t) is band-limited Gaussian noise prior to windowing, whereas win(t) is the time-window function that can be of the trapezoidal or exponential form, as defined by equation (23) (Lam *et al.*, 2000):

$$\mathrm{win}(t) = \mathrm{e}^{-0.4t(6/t_d)} - \mathrm{e}^{-1.2t(6/t_d)}. \tag{23}$$

A different windowing function, as adopted by Boore (2003), is represented by equation (24):

$$\mathrm{win}(t) = 26.312(t/2t_d)^{1.253}\mathrm{e}^{-6.266(t/2t_d)}, \tag{24}$$

$$\mathrm{t_d} = t_{\mathrm{ds}} + t_{\mathrm{dp}}, \tag{25a}$$

$$t_{\mathrm{ds}} = \frac{1}{f_0}, \tag{25b}$$

$$t_{\mathrm{dp}} = b\mathbf{R}, \tag{25c}$$

in which t_d is total ground-motion duration, t_{ds} is source duration, t_{dp} is path duration, f_0 is corner frequency (equals to f_c, if single-corner frequency source model is used as the source model), which is obtained by weighing the two corner frequencies: f_a and f_b, b is fixed at 0.05 at all distances. The final function of t_d can be represented as equation (26):

$$t_d = 0.5\frac{1}{f_a} + 0.5\frac{1}{f_b} + 0.05\mathbf{R}. \tag{26}$$

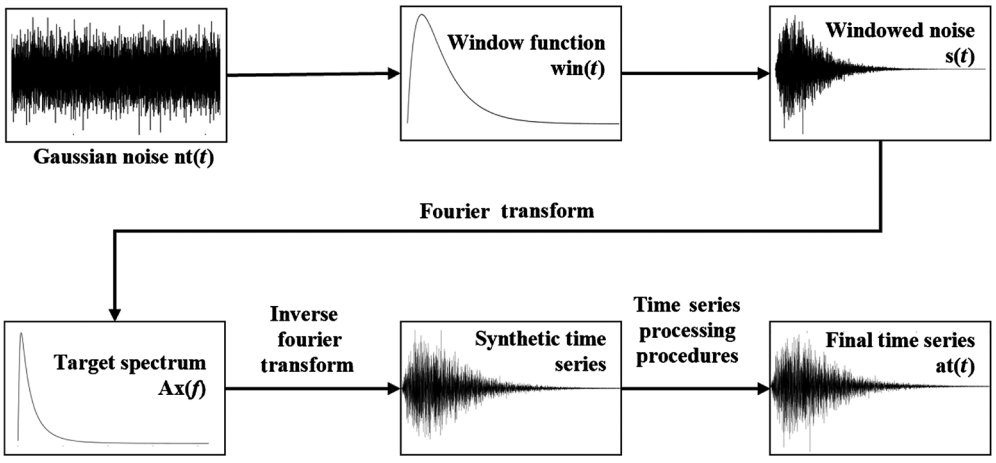

Figure 2. Schematic diagram of ground-motion simulation system (GMSS) illustration.

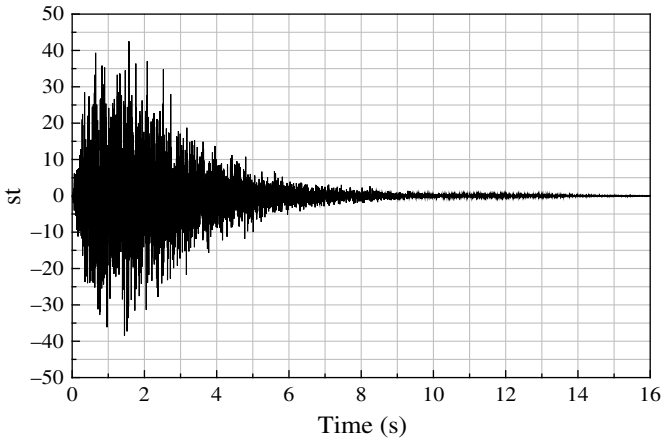

Figure 3. Example windowed noise st(t).

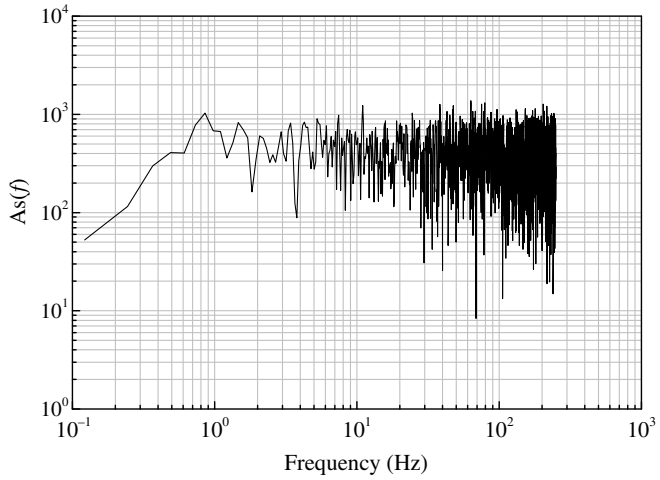

Figure 4. An example Fourier transform of a windowed white noise As(f).

In GMSS, users can opt for the window function win(t), as defined by equation (23), or an alternative specified by the user. The duration function can also be defined by the user for the target region. An example of windowed noise st(t), so generated by GMSS, based on the use of equation (22), is shown in Figure 3.

Fourier transform of windowed noise

Built-in fast Fourier transform function in MATLAB is then used to Fourier transform the windowed white noise, to determine the FAS along with a set of random phase angles. An example FAS is shown in Figure 4.

Filtering the FAS

The seismological model presented in The Makeup of the Seismological Model section is essentially a frequency filter, which is denoted as Ax(f) (as the target Fourier spectrum) that can be used to modify As(f) into Aa(f). The ensemble-averaged Aa(f), as derived from repetitive simulations, displays convergence to Ax(f). The procedure, as described, is preferred to the procedure of filtering white noise prior to windowing (Boore, 2003). Refer Figure 5 that shows an example of the ensemble-averaged Aa(f), in comparison with Ax(f). The example is based on $\Delta\sigma = 200$ bar, $\mathbf{M} = 6$, $\mathbf{R} = 30$ km, $Q_0 = 680$, $n = 0.36$, and no upper-crustal modification was applied in this example.

Generation of time series and time-series processing procedures

To generate ground-motion time series at(t), the set of phase angles obtained from the Fourier transform of st(t) should be made use of in the process of inverse Fourier transform of Aa(f). Time series so derived from the inverse Fourier transform process, as described, can be padded with entries of zero, due to the very nature of the Fourier transform process. It is recommended that the padded time series be preserved and not be stripped away, to avoid distortions of the long-period properties of the simulations (Boore, 2005, 2009). Baseline correction, or zero-order correction, is also required to make corrections for long-period errors in the simulations. Numerical integration is then applied to the acceleration time series, to obtain the respective velocity and displacement time series.

Computation of response spectra

The displacement time series of the single-degree-of-freedom oscillators, in response to base excitations by the simulated

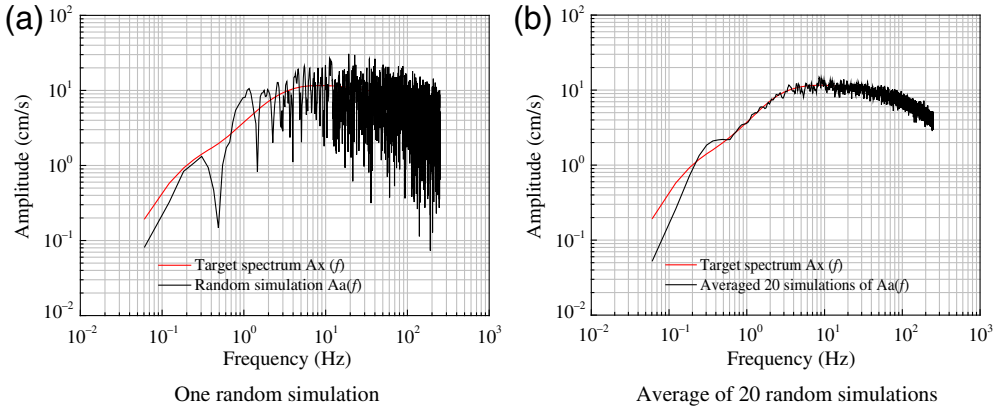

Figure 5. An example of the target spectrum and random simulations. (a) One random simulation and (b) average of 20 random simulations. The color version of this figure is available only in the electronic edition.

time series, can be calculated using time-stepping methods of integration (Chopra, 2007). Central difference method implemented on MATLAB or EXCEL may be applied (Lam *et al.*, 2010).

The user interface of GMSS, showing the generated time series and response spectra, is shown in Figure 6. This user-friendly platform is designed for implementing stochastic ground-motion simulations for multiple engineering purposes. Solid background of engineering seismology is not required to use this platform.

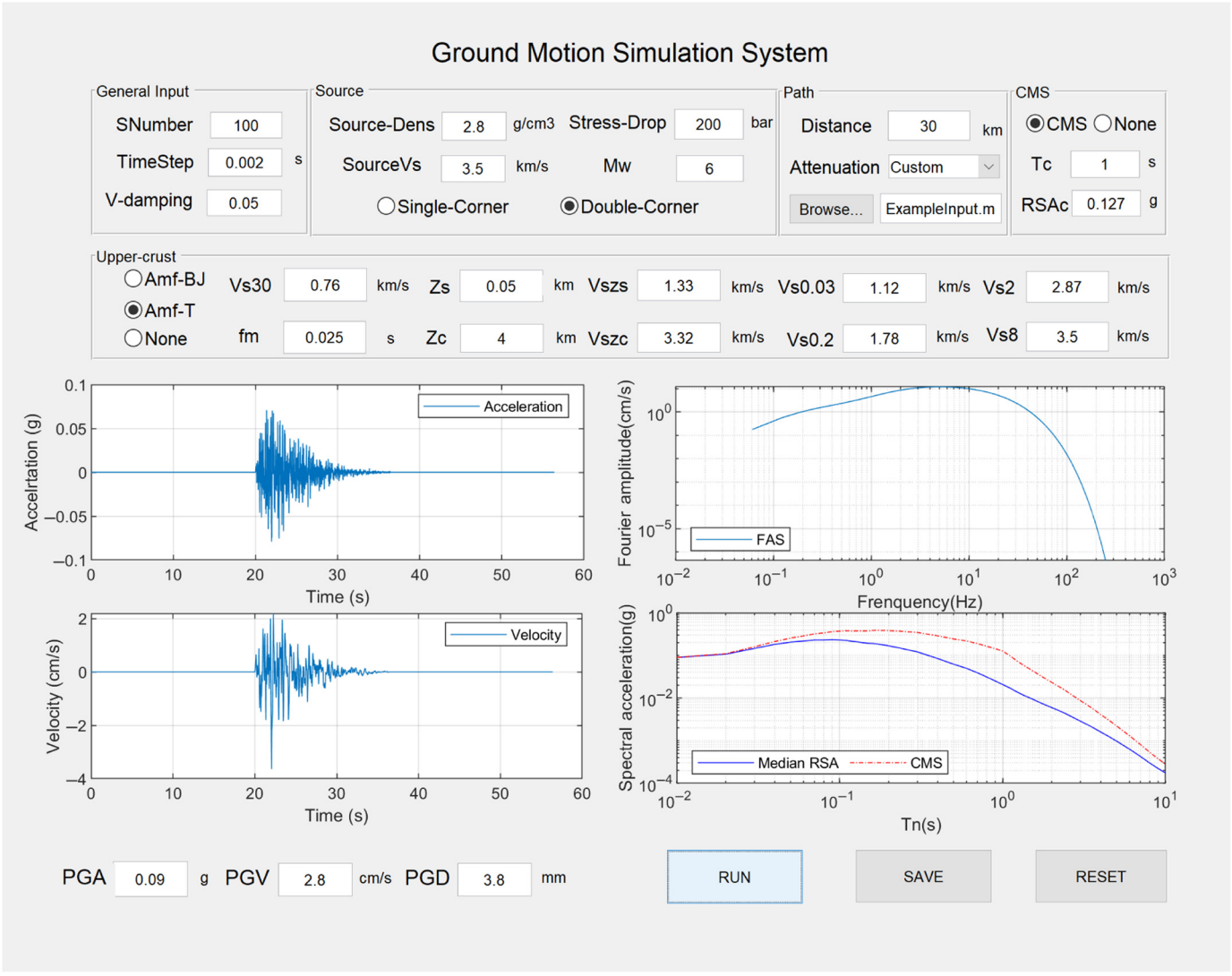

Figure 6. User interface of GMSS. The color version of this figure is available only in the electronic edition.

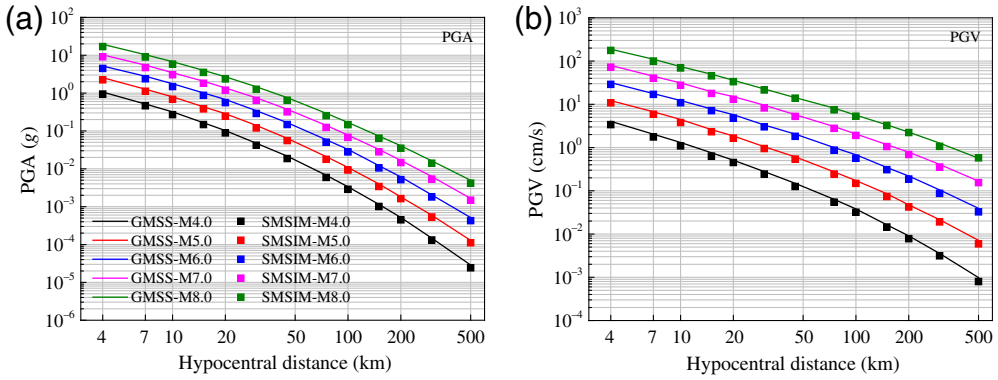

Figure 7. Comparison of predictions from GMSS and Stochastic-Method SIMulation (SMSIM) for peak ground acceleration (PGA) and peak ground velocity (PGV). Solid lines—GMSS and square symbols—SMSIM. (a) PGA and (b) PGV. The color version of this figure is available only in the electronic edition.

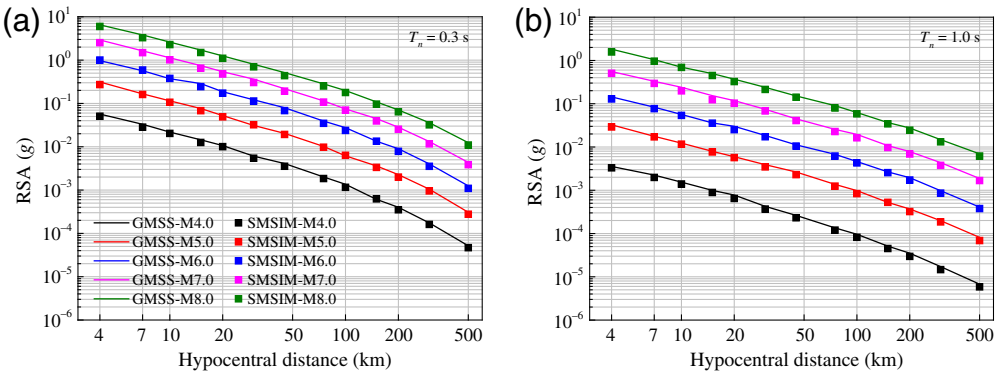

Figure 8. Comparison of predictions from GMSS and SMSIM for response spectral acceleration (RSA) at $T_n = 0.3$ and 1 s. Solid lines—GMSS and square symbols—SMSIM. (a) $T_n = 0.3$ s and (b) $T_n = 1.0$ s The color version of this figure is available only in the electronic edition.

The output of this platform includes time series of the simulated ground motions, peak ground acceleration, peak ground velocity, peak ground displacement, FAS, and response spectra. All the calculation results can be saved into an EXCEL spreadsheet or TXT file, directly by clicking the "SAVE" button. Detailed information, including the programming flowchart, the definition of each symbol shown on the interface, example input and output files, can be found in Data and Resources of this article.

Verification of GMSS by Benchmarking against SMSIM

The computational tool introduced in this article (GMSS) has been validated by comparison with simulations obtained from the use of the widely used program SMSIM (version 7.04), which was originally authored by Boore (2003). The validation was based on the parameters listed in Table 3. The comparisons of peak ground motions reported from the two programs, for a range of **M**–**R** combinations, are presented in Figure 7, whereas the comparisons of the response spectral acceleration at 0.3 and 1.0 s periods are presented in Figure 8. Discrepancies between simulations of the two programs are all within 1%.

The Potential Utility of GMSS

Earthquake ground-motion accelerograms are required for advanced dynamic analysis of a structure experiencing postelastic behavior. Engineering users tend to prefer the use of real recorded accelerograms that can be sourced from an empirical database over the use of synthetic or artificial accelerograms. Many codes of practices typically require only a few (3–7) accelerograms to be incorporated into the dynamic analysis (e.g., Eurocode 8, 2004). However, the required number of accelerograms has been increased to 11 in the 2016 edition of American Society of Civil Engineers (ASCE)-7 (ASCE, 2016). This increase is warranted because of the sensitivity of the response behavior of the structure to the characteristics of individual input ground motion.

It is demonstrated herein that synthetic accelerograms generated by GMSS can contribute to the construction of the conditional mean spectrum (CMS). In other words, a CMS can be constructed from an ensemble mean response spectrum, which is obtained from analyses of synthetic accelerograms, as opposed to the use of a response spectrum specified by ground-motion prediction equations (GMPEs). An outline of the procedure is presented in Table 4.

The PEER NGA-West2 strong-motion database (see Data and Resources) contains 21,539 strong-motion accelerograms, recorded from 599 earthquake events (Ancheta *et al.*, 2014). Accelerograms can be sourced from the PEER database, and have the records selected and scaled in order that the ensemble mean response spectrum is in good agreement with the "target spectrum" that is specified in the user interface of the database. The ground-motion selection procedures are conducted online,

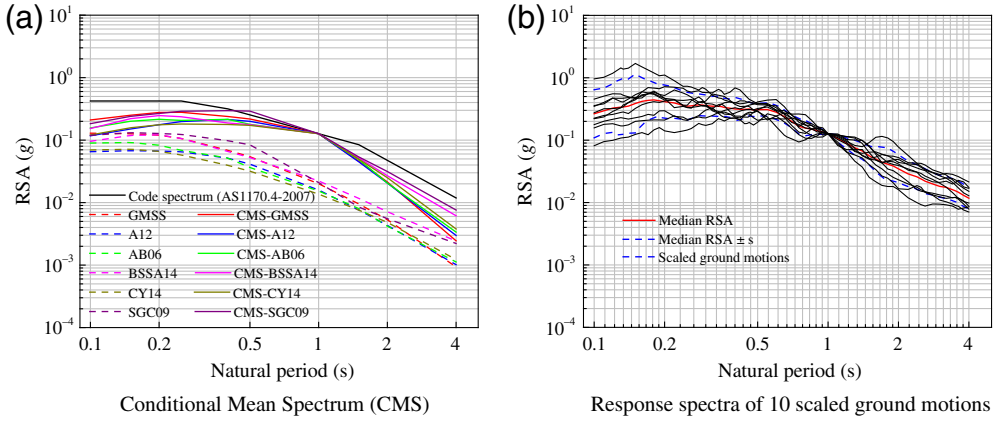

Figure 9. Constructed conditional mean spectrum (CMS) and response spectra of 10 scaled ground motions retrieved from Pacific Earthquake Engineering Research Center (PEER) Next Generation Attenuation 2 (NGA-West2) database. (a) CMS and (b) response spectra of 10 scaled ground motions. A12, Allen (2012); AB06, Atkinson and Boore (2006); BSSA14, Boore, Stewart, *et al.* (2014); CY14, Chiou and Youngs (2014); SGC09, Somerville *et al.* (2009). The color version of this figure is available only in the electronic edition.

using the tool provided by the PEER database (see Data and Resources). A CMS can be used as a target spectrum, as per recommendations by Baker (2011).

In constructing a CMS, it is also required to determine a dominant scenario for a specified reference period (conditioning natural period [Tc]), and this involves probabilistic seismic-hazard analysis followed by hazard disaggregation. The example earthquake scenario (M6R40) used herein for illustration was based on sourcing information presented in Tang (2019). The CMS so derived from GMSS for the scenario of M6R40 is shown in Figure 9a (detailed information of GMPEs is shown in Table 5), along with a code-specified response spectrum (The code spectrum of AS1170.4-2007 was used in the illustration.). To complete the illustration to demonstrate its viability, response spectra calculated from 10 of the retrieved and scaled accelerograms are also shown (Fig. 9b). Their respective ground-motion acceleration time series (along with the recording sequence number [RSN]) are shown in Figure 10.

Summary and Conclusion

This article is aimed at introducing GMSS as an open-source MATLAB software package, for implementing stochastic simulations of earthquake ground motions. The distinctive feature of GMSS is that it presents alternative methods of modeling crustal SWV profile kilometers into bedrock and has the modeled profile incorporated into the ground-motion simulations using the seismological model as a framework.

In addition to synthesizing accelerograms on rock for any given earthquake scenario, as defined by the magnitude–distance combination, GMSS includes facilities for calculating response spectra and median predictions of ground-motion

TABLE 3
Parameter Values Used in Stochastic Simulations for Comparison Purpose

Parameter	Input Value
Source SWV	3.8 km/s
Source density	2.8 g/cm^3
Source model	Equation (7a–c)
Spectral sag	$\varepsilon = 10^{0.605-0.255\mathbf{M}}$
Moment magnitude	**M** = 4.0–8.0
Distance	**R** = 4.0–500 km
Geometric spreading	$\mathbf{R}^{-1}$
Stress drop	$\Delta\sigma$ = 200 bars
Anelastic attenuation	$680f^{0.36}$
Timestep	dt = 0.002 s
Number of simulations	50

SWV, shear-wave velocity.

TABLE 4
Outline of Procedure for the Use of Ground-Motion Simulation System (GMSS) to Construct Conditional Mean Spectrum (CMS)

Step	Input Information	Output Information
1	Results of probabilistic seismic-hazard analysis and hazard disaggregation	Dominant earthquake scenarios defined by **M–R** combinations
2	Input parameters into GMSS as shown in Figure 6	Synthetic accelerograms for given **M–R** combinations and regional crustal conditions
3	Synthetic accelerograms for a given **M–R** combination	Median response spectrum estimated for a given **M–R** combination
4	Modifications to the median response spectrum estimate for a given **M–R** combination	CMS as the target spectrum
5	Target spectrum as input into the user interface of database of recorded accelerograms	An ensemble of selected and scaled recorded accelerograms

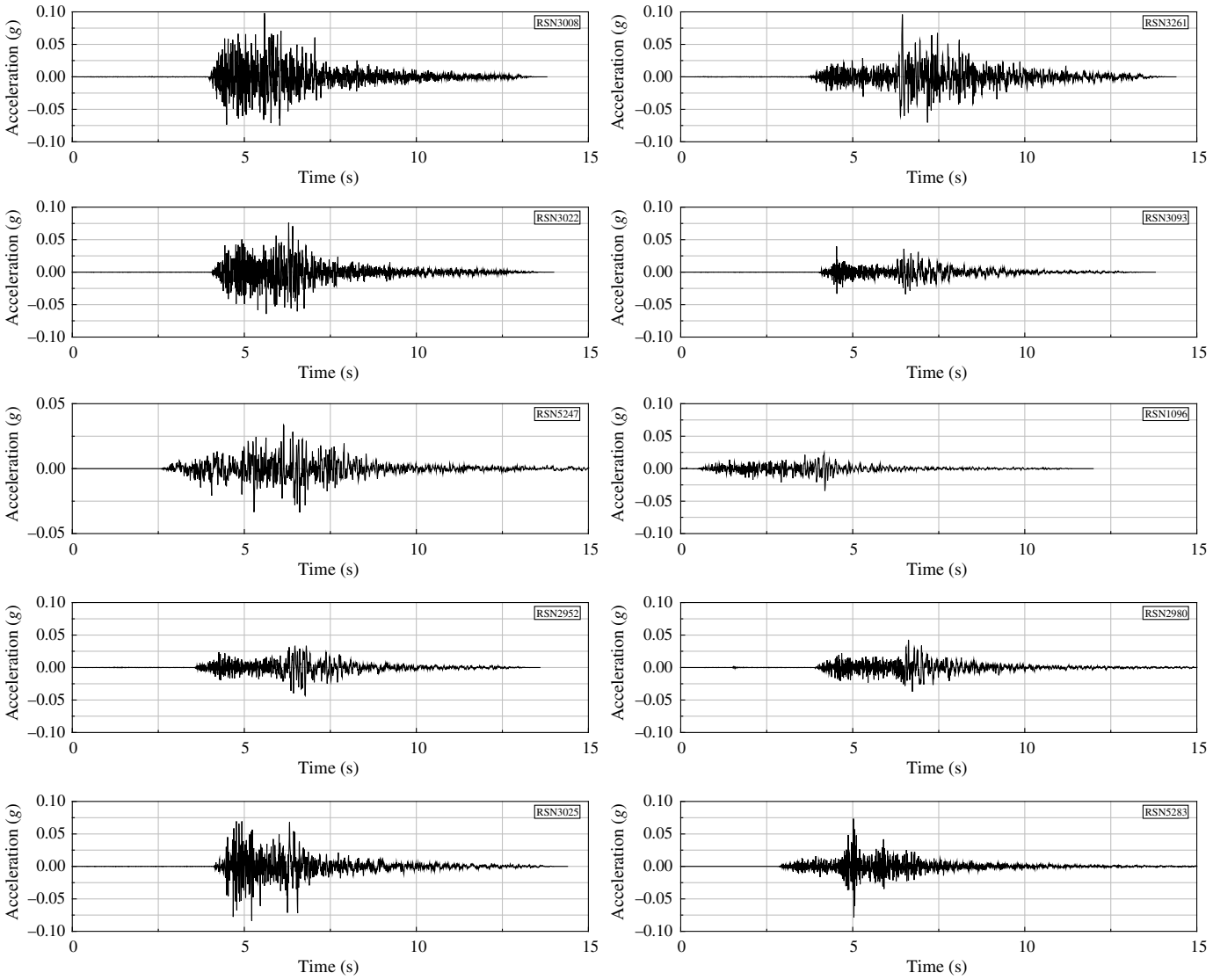

Figure 10. Scaled time series of 10 ground motions retrieved from PEER NGA-West2 database.

parameters associated with the time series (Tang *et al.*, 2019, 2020).

This article is also aimed at encouraging users who have programming skills to develop their computational tools that incorporate their updates to the seismological model. Thus, enough up-to-date information on seismological modeling and on time-series simulations has been presented, for ease of reference by readers in one article. The accuracies of GMSS have been verified by comparison of the generated peak ground motions as well as the response spectra against those generated by program SMSIM. Enough details of the verifications are presented with a view of providing the benchmarks to guide the development of similar computational tools in the future.

Toward the end of this article, readers are enlightened to the potential utility of GMSS as a transdisciplinary tool for facilitating the sourcing and scaling of accelerograms from a strong-motion database of real earthquake records, for use in engineering design of a critical structure, and this involves constructing CMS.

TABLE 5
List of Ground-Motion Prediction Equations (GMPEs) for Constructing Conditional Mean Spectrum (CMS)

GMPEs	References
A12 (noncratonic)	Allen (2012)
AB06	Atkinson and Boore (2006)
BSSA14	Boore, Stewart, *et al.* (2014)
CY14	Chiou and Youngs (2014)
SGC09 (noncratonic)	Somerville *et al.* (2009)

Data and Resources

The ground-motion simulation system (GMSS) software package can be downloaded from the GitHub page of Y. T. (https://github.com/Y-Tang99/GMSS1.0, last accessed October 2020). The Stochastic-Method SIMulation (SMSIM) software can be downloaded from David Boore's website page (http://www.daveboore.com/, last accessed April 2020). The information about Pacific Earthquake Engineering Research Center (PEER) Next Generation Attenuation-East Project (NGA-East) strong-motion database is available at https://ngawest2.berkeley.edu (last accessed September 2020). MATLAB is available at www.mathworks.com/products/matlab (last accessed May 2020).

Acknowledgments

The financial contribution of the Commonwealth Government of Australia through the Cooperative Research Centre Program is gratefully acknowledged. The assistance provided by Elisa Lumantarna at The University of Melbourne, in related research work, is acknowledged. The valid and constructive comments given by both anonymous reviewers and Editor-in-Chief Allison Bent are highly acknowledged.

References

Abercrombie, R. E. (1997). Near-surface attenuation and site effects from comparison of surface and deep borehole recordings, *Bull. Seismol. Soc. Am.* **87,** no. 3, 731–744.

Allen, T. I. (2012). *Stochastic Ground-Motion Prediction Equations For Southeastern Australian Earthquakes Using Updated Source And Attenuation Parameters*, Geoscience Australia, Canberra, Australia, 69 pp.

American Society of Civil Engineers (ASCE) (2016). Minimum design loads and associated criteria for buildings and other structures, (ASCE/SEI 7-16), available at https://www.asce.org/ (last accessed October 2018).

Ancheta, T. D., R. B. Darragh, J. P. Stewart, W. J. Silva, E. Seyhan, B. S.-J. Chiou, K. E. Wooddell, R. W. Graves, A. R. Kottke, D. M. Boore, *et al.* (2014). NGA-West2 database, *Earthq. Spectra* **30,** no. 3, 989–1005.

Atkinson, G. (1993). Earthquake source spectra in eastern North America, *Bull. Seismol. Soc. Am* **83,** 1778–1798.

Atkinson, G. M., and D. M. Boore (1995). Ground-motion relations for eastern North America, *Bull. Seismol. Soc. Am.* **85,** 17–30.

Atkinson, G. M., and D. M. Boore (2006). Earthquake ground-motion prediction equations for eastern North America, *Bull. Seismol. Soc. Am.* **96,** no. 6, 2181–2205.

Atkinson, G. M., and D. M. Boore (2014). The attenuation of Fourier amplitudes for rock sites in eastern North America, *Bull. Seismol. Soc. Am.* **104,** 513–528.

Atkinson, G. M., and W. J. Silva (2000). Stochastic modeling of California ground motions, *Bull. Seismol. Soc. Am.* **90,** no. 2, 255–274.

Baker, J. W. (2011). Conditional mean spectrum: Tool for ground-motion selection, *J. Struct. Eng.* **137,** no. 3, 322–331.

Boore, D. (1983). Stochastic simulation of high-frequency ground motions based on seismological models of the radiated spectra, *Bull. Seismol. Soc. Am.* **73,** 1865–1894.

Boore, D. M. (2003). Simulation of ground motion using the stochastic method, *Pure Appl. Geophys.* **160,** 635–676.

Boore, D. M. (2005). On pads and filters: Processing strong-motion data, *Bull. Seismol. Soc. Am.* **95,** no. 2, 745–750.

Boore, D. M. (2009). Comparing stochastic point-source and finite-source ground-motion simulations: SMSIM and EXSIM, *Bull. Seismol. Soc. Am.* **99,** no. 6, 3202–3216.

Boore, D. M. (2013). The uses and limitations of the square-root-impedance method for computing site amplification, *Bull. Seismol. Soc. Am.* **103,** no. 4, 2356–2368.

Boore, D. M. (2015). *Point-Source Stochastic-Method Simulations of Ground Motions for the PEER NGA-East Project*, Pacific Earthquake Engineering Research Center, Berkeley, California, 39 pp.

Boore, D. M. (2016). Short note: Determining generic velocity and density models for crustal amplification calculations, with an update of the Boore and Joyner (1997) generic amplification for $V_s(Z) = 760$ m/s, *Bull. Seismol. Soc. Am.* **106,** no. 1, 316–320.

Boore, D. M., and S. Akkar (2003). Effect of causal and acausal filters on elastic and inelastic response spectra, *Earthq. Eng. Struct. Dynam.* **32,** 1729–1748.

Boore, D. M., and W. B. Joyner (1997). Site amplifications for generic rock sites, *Bull. Seismol. Soc. Am.* **87,** no. 2, 327–341.

Boore, D. M., C. D. Alessandro, and N. A. Abrahamson (2014). A generalization of the double-corner-frequency source spectral model and its use in the SCEC BBP validation exercise, *Bull. Seismol. Soc. Am.* **104,** no. 5, 2387–2398.

Boore, D. M., K. W. Campbell, and G. M. Atkinson (2010). Determination of stress parameter for eight well-recorded earthquakes in eastern North America, *Bull. Seismol. Soc. Am.* **100,** 1632–1645.

Boore, D. M., J. P. Stewart, E. Seyhan, and G. M. Atkinson (2014). NGA-West2 equations for predicting PGA, PGV, and 5% damped PSA for shallow crustal earthquakes, *Earthq. Spectra* **30,** no. 3, 1057–1085.

Brocher, T. M. (2005). Empirical relations between elastic wavespeeds and density in the Earth's crust, *Bull. Seismol. Soc. Am.* **95,** no. 6, 2081–2092.

Brune, J. N. (1970). Tectonic stress and the spectra of seismic shear waves from earthquakes, *J. Geophys. Res* **75,** 4997–5009.

Chandler, A. M., N. T. K. Lam, and H. H. Tsang (2005). Shear wave velocity modelling in crustal rock for seismic hazard analysis, *Soil Dynam. Earthq. Eng.* **25,** 167–185.

Chandler, A. M., N. T. K. Lam, and H. H. Tsang (2006). Near surface attenuation modelling based on rock shear wave velocity profile, *Soil Dynam. Earthq. Eng.* **26,** 1004–1014.

Chen, S. (2000). Global comparisons of earthquake source spectra, *Ph.D. Thesis*, Carleton University, Ottawa, Canada.

Chiou, B. S. J., and R. R. Youngs (2014). Update of the Chiou and Young's NGA model for the average horizontal component of peak ground motion and response spectra, *Earthq. Spectra* **30,** no. 3, 1117–1153.

Chopra, A. K. (2007). *Dynamics of Structures Theory and Applications to Earthquake Engineering*, Third Edition, Pearson Education Inc., Hoboken, New Jersy, 171–173.

Eurocode 8 (2004). *Design of structures for earthquake resistance—Part 1: General rules, seismic actions and rules for buildings*, EN 1998-1:2004 European Committee for Standardisation, United Kingdom.

Goulet, C. A., T. Kishida, T. D. Ancheta, C. H. Cramer, R. B. Darragh, and W. J. Silva (2014). *PEER NGA-East Database*,

Pacific Earthquake Engineering Research Center, Berkeley, California.

Hanks, T. C., and H. Kanamori (1979). A moment magnitude scale, *J. Geophys. Res.* **84,** no. B5, 2348–2350.

Lam, N. T. K., J. Wilson, and G. Hutchinson (2000). Generation of synthetic earthquake accelerograms using seismological modelling: A review, *J. Earthq. Eng.* **4,** no. 3, 321–354.

Lam, N. T. K., J. Wilson, and E. Lumantarna (2010). Modelling seismically induced storey drift in buildings, *Int. J. Struct. Eng. Mech.* Invited paper, **35,** no. 4, 459–478.

Motazedian, D., and G. M. Atkinson (2005). Stochastic finite-fault modeling based on a dynamic corner frequency, *Bull. Seismol. Soc. Am.* **95,** no. 3, 995–1010.

Somerville, P., R. Graves, N. Collins, S. G. Song, S. Ni, and Phil R. Cummins (2009). Source and ground motion models for Australian earthquakes, *2009 Conf. of the Australian Earthquake Engineering Society*, Newcastle, Australia, 11–13 December.

Tang, Y. (2019). Seismic hazard analysis and management for low-to-moderate seismicity regions based on ground motion simulation, *Ph.D. Thesis*, The University of Melbourne, Melbourne, Australia.

Tang, Y., N. T. K. Lam, H. H. Tsang, and E. Lumantarna (2019). Use of macro-seismic intensity data to validate a regionally adjustable ground motion prediction model, *Geosciences* **9,** no. 10, 1–22, doi: 10.3390/geosciences9100422.

Tang, Y., N. T. K. Lam, H. H. Tsang, and E. Lumantarna (2020). An adaptive ground motion prediction equation for use in low-to-moderate seismicity regions, *J. Earthq. Eng.* doi: 10.1080/13632469.2020.1784810.

Yenier, E., and G. M. Atkinson (2014). Equivalent point-source modeling of moderate-to-large magnitude earthquakes and associated ground-motion saturation effects, *Bull. Seismol. Soc. Am.* **104,** no. 3, 1458–1478.

Manuscript received 17 June 2020
Published online 25 November 2020